Front. Mater. Sci. 2016, 10(2): 122–133
DOI 10.1007/s11706-016-0333-0

RESEARCH ARTICLE

Comparative evaluation of a biomimic collagen/hydroxyapatite/β-tricaleium phosphate scaffold in alveolar ridge preservation with Bio-Oss Collagen

Tong WANG[1*], Qing LI[2,1,3*], Gui-feng ZHANG[4], Gang ZHOU[5], Xin YU[5], Jing ZHANG[5], Xiu-mei WANG[6], and Zhi-hui TANG (✉)[1,3]

1 The 2nd Dental Center, Peking University School and Hospital of Stomatology, Beijing 100101, China
2 Center of Digital Dentistry, Peking University School and Hospital of Stomatology, Beijing 100081, China
3 National Engineering Laboratory for Digital and Material Technology of Stomatology, Beijing 100081, China
4 Institute of Process Engineering, Chinese Academy of Sciences, Beijing 100190, China
5 Key Laboratory for Biomechanics and Mechanobiology of Ministry of Education, School of Biological Science and Medical Engineering, Beihang University, Beijing 100191, China
6 Institute of Regenerative Biomaterials, Tsinghua University, Beijing 100084, China

ABSTRACT: Bone scaffolds are critical in current implant and periodontal regeneration approaches. In this study, we prepared a novel composite type-I collagen and hydroxyapatite (HA)/β-tricaleium phosphate (TCP) scaffold (CHTS) by incorporating type-I collagen and bovine calcined bone granules, prepared as a mixture of 50% HA and 50% TCP, by freeze drying. We then characterized the CHTS and determined its cytotoxic effects. Additionally, ridge preservation experiments were carried out to evaluate the clinical effects of the CHTS. The results demonstrated that the composite scaffolds had good surface morphology and no cytotoxicity. Additionally, an *in vivo* experiment in an animal model showed that the CHTS performed equally as well as Bio-Oss Collagen, a widely used bone graft in ridge preservation. These findings revealed that the CHTS, which contained natural constituents of bone, could be used as a scaffold for bone regeneration and clinical use.

KEYWORDS: hydroxyapatite; β-tricaleium phosphate (TCP); collagen; scaffold; ridge preservation

Contents

Received December 5, 2015; accepted February 29, 2016

E-mail: tang_zhihui@live.cn

* T.W. and Q.L. contributed equally to this work.

1 Introduction

With the development of dental implantology, the rates of successful implant-supporting dentures have reached over 95% among adults, and implant therapy is being widely accepted by an increasing number of patients [1–2]. Importantly, achieving an adequate bone volume in the implant site is necessary for the success of implant surgery and the related aesthetics of gum soft tissue [3–4]. However, alveolar bone shrinks extremely rapidly after extraction; indeed, a previous study showed that the buccal bone will decrease in size by 1.24–1.67 mm in 6 months [5–7]. Many studies have shown that bone grafting in the socket at the time of tooth extraction will ameliorate inadequate bone growth; thus, alveolar ridge preservation can be achieved by conservation of bone volume and shortening the cycle of treatment [4,8–11].

Because of the disadvantages of autografts and allografts, artificial bone substitutes have become a major focus of bone tissue engineering, and various types of composite materials have been developed. For example, porous ceramics have been manufactured for use in bone tissue engineering; however, these materials have poor mechanical features and an inferior ability to promote bone regeneration [12]. An ideal bone scaffold should be absorbed and replaced by autologous cells and tissue and should have a reasonable degradation rate [13]. Moreover, ideal materials should have strong mechanical properties and a porous structure in order to guarantee the retention of scaffolds, satisfy the clinical requirements of biomaterials, and provide space for cell proliferation and adhesion [14–15].

Hydroxyapatite (HA) and β-tricalcium phosphate (TCP) have superior biocompatibility and osteoconductivity and thus have been widely used in orthopedic and maxillofacial surgeries [16]. Many approaches have also been applied to improve the osteogenic and mechanical properties of these materials, including growth factor addition, electrospinning, nanotechnology, magnetic field application, and three-dimensional (3D) printing [17–20]. The combination of HA with TCP is expected to achieve improved characteristics owing to the differential effects of these two components on the regeneration process; that is, HA can provide a cell matrix and improve the mechanical strength of the material, whereas TCP can influence the earlier stages of bone formation by creating an optimal environment before being absorbed [21]. This combination is expected to also have several additional advantages, including the absence of donor morbidity, biocompatibility due to the chemical similarity of the materials with the host bone, and lack of anomalous inflammatory reactions [22]. Additionally, by controlling the proportion of each component, the bioactivity and biodegradation could be manipulated [22]. For example, the molar ratio of n(HA):n(β-TCP) = 30:70 could achieve better clinical results than that of n(HA):n(β-TCP) = 70:30 [23]. However, organism calcified tissues have superiority because of their organic matrix, particularly collagen type I, which exhibits improved mechanical properties and bioactivity. Hence, the incorporation of organic and inorganic components may enhance the properties of biomaterials greatly [24].

Collagen, which is the main component of the extracellular matrix (ECM), is a well-studied natural polymer used in tissue engineering scaffolds [25]. Collagen has been widely used in the clinical setting for many years and exhibits good biodegradability, biocompatibility, and absorbability [26] and is close to the natural organic structure of bone, which would exert positive effects on cell fates [27]. Collagen can also facilitate cell attachment and can be easily absorbed by organisms [27]. Moreover, collagen can inhibit the growth of bacterial pathogens [28]. Therefore, collagen may be a promising organic material for incorporation with HA and TCP. Such composite materials, mimicking the natural composition of bones, may be biologically compatible, exhibiting proper porosity and interconnected porous structures to enhance the proliferation of cells [29–30]. Additionally, these composites would be expected to have better mechanical

properties than the individual components, including improved stability [31] and mechanical 'wet' properties [32]. Composite materials containing HA, TCP, and collagen could augment the recruitment of progenitor cells and their differentiation due to the adhesion properties of collagen and the osteoconductive ability of mineral composition [33].

After tooth extraction, the site will experience obvious resorption, which will lead to insufficient bone volume and difficulty in implantation and prosthetic treatment [9–11]. Clinicians prefer to conduct bone grafting in the sockets; this technique may slow bone resorption and result in increased bone preservation. Studies have shown that this biomaterial exhibits promising effects to the contribution of new bone formation [10,34–35].

Among all bone graft, Bio-Oss Collagen, which consists of 90% mineralized bovine bone matrix (carbapatite and hydroxyapatite) and 10% porcine collagen (type-I), has acquired satisfactory clinical effects so far due to its excellent porous structure, biocompatibility and similar components with natural bone. Nevins et al. revealed the regeneration of the periodontal attachment apparatus in human periodontitis bony defects with Bio-Oss Collagen graft [36]. Cardaropoli et al. treated the infrabony defects using Bio-Oss collagen combined with orthodontic movement [37]. In the study reported by Heinemann et al., they conducted Bio-Oss graft in the extraction sockets with implantation and achieve better effects than graft only or none graft [38].

In this study, we aimed to explore a novel solution dispersion approach to synthesize a highly bioactive collagen/bovine bone (HA + TCP) composite scaffold (CHTS). We also examined the surface characteristics and composition of the CHTS and compared them with the Bio-Oss Collagen biomaterial. In order to investigate the biocompatibility of the CHTS and gain further insights into the potential clinical applications of the CHTS, we also tested *in vitro* cell proliferation and *in vivo* ridge preservation.

2 Materials and methods

2.1 Preparation of CHTS

2.1.1 Preparation of bovine bone powder

The cancellous portion of bovine humerus epiphysis was cut into cubes with dimensions of 4 mm × 4 mm × 10 mm. After being incubated in sodium hydroxide and hydrogen peroxide solution for 30 min, the bone cubes were then incubated at 103.4 kPa for 1 h to remove collagen and proteins. The bone scaffolds were washed in deionized water and dried overnight at 60°C. Next, the bone scaffolds were placed into a muffle furnace, slowly heated to 700°C [17,39], and calcined in an oxygen atmosphere for 2 h. The calcined scaffolds were then immersed in 0.09 mol/L sodium acid pyrophosphate water solution for 72 h in a water bath at 70°C. The drying process was repeated, and the scaffolds were placed into the muffle furnace again and slowly heated to 1200°C for 1 h [40]. After heating, the scaffolds were ground, and the product was filtered through a screen cloth to obtain calcined bone particles with a diameter of 0.25–1 mm.

2.1.2 Preparation of collagen–bone particle composite scaffolds (CHTSs)

The preparation of the composite material was carried out using a freeze-drying approach [41]. In order to avoid inflammation and other negative effects of acid material, collagen was dispersed in pure water. Fibrillary high-purity collagen (Collagen Biotechnology Co., Ltd, China) was dispersed in distilled water at a concentration of 4 g/100 mL. To achieve an ideal dispersion, a homogenizer (I KA, Germany) was applied. After the collagen was sufficiently mixed with water, the bone particles were mixed with the collagen slurries under constant stirring at a speed of 45 r/min in order to disperse the bone particle homogeneously. The concentration of bone particles was 36 g/100 mL. The solution was then degassed and injected into stainless steel molds with dimensions of 5 mm × 5 mm × 10 mm. In order to condense the material, the slurries were subjected to a constant pressure of 105 kPa for 2 h. The molds were then incubated at −10°C to freeze for 2 h, and the solution was then freeze-dried in a vacuum to obtain the porous CHTS. The scaffolds were gamma irradiated at 25 kGy for sterilization at room temperature.

2.2 Scaffold analysis

2.2.1 Scanning electron microscopy (SEM)

SEM was performed on a Hitachi S-4800 SEM (Hitachi, Japan). The specimens were fixed in 2.5% glutaraldehyde in water for 2 h and then dehydrated with gradient alcohol. After critical point drying, the morphology of the specimens was observed.

2.2.2 Element analysis (EDX spectra)

An energy dispersive X-ray (EDX) spectrometer (Hitachi S-4800), which was connected to the SEM, was applied to determine the elemental composition of CHST. The specimen preparation was the same as that described in Section 2.2.1. The results and graphs were generated using JEOL and SwiftED-1.ipj software.

2.2.3 FTIR measurements

FTIR measurements were performed with a Shimadzu FTIR-8400S (Shimadzu, Japan) to acquire information about the chemical structure. The spectral range was set to 4000–400 cm^{-1} with a resolution of 2 cm^{-1} and scan number of 32 times. The samples were diluted to 1% by mixing with KBr (IR grade). The mixture was compressed using a mechanical pressing system at 10 tons.

2.2.4 X-ray diffraction (XRD) analysis

In order to examine the crystal phase composition of the samples, XRD was conducted. An area (0.5 mm × 0.5 mm) of each sample was randomly selected, and the XRD spectra were acquired at room temperature with a Siemens D500 series diffractometer (Siemens, Germany) using Cu Kα radiation. The range was 10°–90° with 0.02° steps and 1 s/step scan speed.

2.3 Biological evaluations of scaffolds *in vitro*

2.3.1 Cell culture

The cytotoxicity of the CHTS was analyzed by assessment of MC3T3-E1 cell proliferation. MC3T3-E1 pre-osteoblasts (Sciencell, USA) were cultured in 100-mm dishes with alpha minimum essential medium (α-MEM; Gibco, USA) supplemented with 10% (v/v) fetal bovine serum (FBS; Gibco), 1% (v/v) l-glutamine (Invitrogen Corp., Carlsbad, CA, USA). The medium was replaced every other day. Cells were digested using a trypsin-EDTA solution (Sigma, St. Louis, MO, USA), and the cell number was determined using a hemacytometer. The cell suspension was centrifuged for 5 min at 1200 r/min at room temperature and resuspended in α-MEM containing 10% FBS to a density of 1×10^7 cells/mL. Collagen scaffolds (CHTSs and Bio-Oss Collagen) were placed into 24-well tissue culture plates (Corning, USA). Each scaffold sample was then seeded with 200 μL cell suspensions. The atmosphere was maintained at 37°C with 5% CO_2. After 1 h to allow cell adhesion, 700 μL α-MEM containing 10% FBS was added to each well. The medium was replaced every other day.

2.3.2 Cell proliferation assays

Cell proliferation was determined using MTT assays after culture for 1, 3, 5, or 7 d. In brief, each well was aspirated and washed with phosphate-buffered saline (PBS) three times. Next, 700 μL of α-MEM containing 10% FBS and 70 μL MTT (0.5 mg/mL in water) was added to each well. The plates were then incubated at 37°C with 5% CO_2 for 3 h in the dark. The medium was removed, and 700 μL DMSO (Sigma) was added to each well to dissolve the formed formazan crystals. After shaking gently on a shaker in the dark for 15 min, the absorbance at 450 nm was measured with a microplate reader (Bio-kinetics reader; Bio-Tek Instruments, USA). Measurements were repeated in triplicate for each respective group.

2.4 Biological evaluations of scaffolds *in vivo*

2.4.1 Tooth extraction and ridge preservation

The osteogenic abilities of the scaffolds in vivo were evaluated by ridge preservation in Beagle dogs. The Ethical Committee of Peking University approved the research protocol. Two beagle dogs (age, approximately 12–18 months; weight, 10–14 kg) were used in this study. Before surgery, teeth were cleaned with 0.12% chlorhexidine solution, and tooth brushing was performed for both dogs. The dogs were anesthetized by intravenous injection of 30 mg/kg pentobarbital sodium, and local anesthesia was carried out with articaine hydrochloride. The bilateral mandible premolars (P1, P2, and P3) as well as the upper and lower incisors (L1, L2, L3) were randomly extracted with little damage to the walls of the sockets. The mucoperiosteal flap was elevated to expose the alveolar ridge crest. Each tooth was extracted individually with dental forceps and dental elevators (the premolar crown was hemisectioned in advance). The mandibular P1, P2, and P3 were used for histological evaluation, and the other teeth were used for ridge preservation. A randomization scheme was generated using a random number table, and in upper and lower L1, L2, L3 and maxillary P1, P2, and P3 sites, nine of which were randomly chosen and divided into three groups; three of the sockets were filled with CHTSs after curetting of the sockets, three were filled with Bio-Oss Collagen, and the remaining sockets were used as negative controls without any grafts (Fig. 1). The flaps were

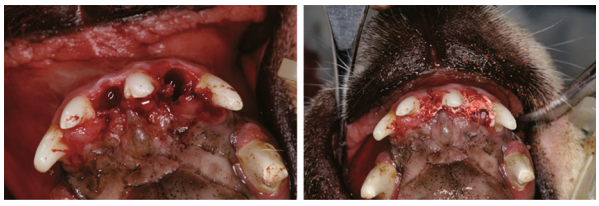

Fig. 1 Tooth extraction and graft filling.

repositioned with interrupted sutures using 4-0 nonabsorbable sutures. For postsurgical care, animals were fed a soft diet and received 25 mg/kg amoxicillin (Baiyunshan, China). The oral hygiene maintenance using 0.12% chlorhexidine solution was performed for 7 d after surgery.

2.4.2 Cone beam computed tomography (CBCT) examination

Before the operation and 2 months after the operation, CBCT (LargeV, China) scans with 0.25-mm-thick layers were performed in order to determine the dimensional variation in the alveolar sockets. SmartV software was used to measure the alveolar bone. The basis nasi was used as the maxillary reference plane, and the mandibular bone lower edge was used as the mandibular reference plan. To determine the height of the alveolar bone in the sagittal slice, the long axis of the alveolar bone was adjusted parallel to the adjacent tooth's long axis (Fig. 2(a)). Then, from the corresponding coronal slice, the distance from the reference plane to the alveolar bone crest was defined as the height of the alveolar bone at that site (Fig. 2(b)). In the measurement of alveolar bone width, the same reference plane and sagittal slice were adopted. From the coronal slice, the axial slice was shifted to a position whose distance to the reference plane was a fixed value (9, 10, or 11 mm; Fig. 2(c)). Then, from the axial slice, the width of the alveolar bone was measured from the buccal lamella to the palatal (Fig. 2(d)). The differences in height and width between the two examinations at the same site were defined as ΔHR and ΔWR, respectively. The bone density was also determined using Hounsfield units (HU).

2.4.3 Preparation of defects and scaffold implantation

In order to evaluate the tissue variation histologically, the dogs were subjected to the same anesthesia process 3 months after implantation. An "H" shape incision was made in the mandible edentulous alveolar process in the premolar-molar region of the side between the canine tooth and the fourth premolar (P4). A muco-periosteal flap was

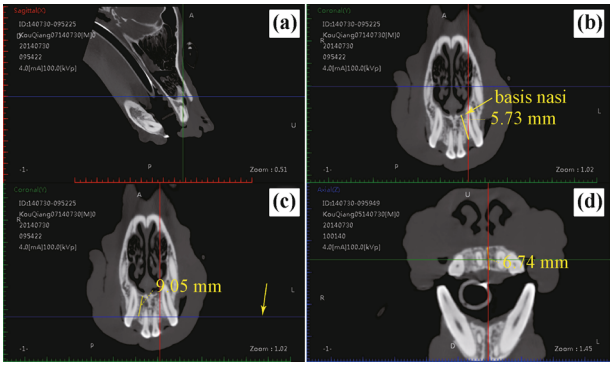

Fig. 2 CBCT images showing the process of measurement of alveolar bone height and width. **(a)** By rotating and shifting the image, the long axis of the alveolar bone (determined from the long axis of the adjacent tooth) was adjusted to parallel with the green line (coronal slice). **(b)** The coronal slice. The yellow line indicates the reference plane, and the height of the alveolar bone. **(c)** At the same sagittal position, the blue line (axial slice) was shifted to make the distance between the axial slice and reference plane a certain value (9, 10 or 11 mm). **(d)** The axial slice. The yellow line indicates the width of the alveolar bone.

elevated, and three defect holes were prepared in the middle of the alveolar ridge crest with an ITI implant system (Strauman, Switzerland). A randomization scheme was generated using a random number table. Each hole was prepared to the dimension of Φ3.5 mm × 10 mm with a drill, and the holes were irrigated with cold normal saline. These holes served as bone defects with dimension of Φ3.5 mm × 10 mm. Overall, every dog had three defects on each side of the mandible (total of six defects for each dog). CHTSs and Bio-Oss Collagen were used to fill two random defects each, and the remaining two defects were used as blank controls filled with blood clots. After irrigation with normal saline, the flaps were repositioned with interrupted sutures using 4-0 nonabsorbable sutures (Fig. 3).

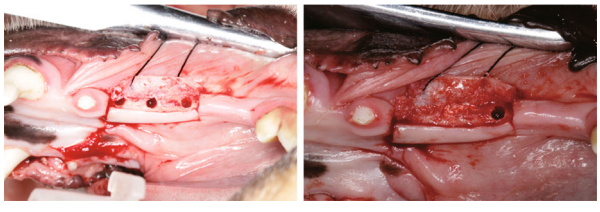

Fig. 3 Bone defects preparation and bone graft filling.

After healing for 60 d, the dogs were euthanized by an overdose of sodium pentobarbitone administered intravenously. After removal of the soft tissue, both jaws were sawed off and cut into blocks using dental handpieces and diamond burs. The blocks were then fixed in a solution containing a mixture of 5% glutaraldehyde and 4% formaldehyde [42].

2.4.4 Histological evaluation

The blocks were dehydrated in a gradient series of alcohols (50%, 70%, 90%, 95%, 100%, and 100%) and then infiltrated in methacrylate, polymerized, and sectioned at the vertical plane of the mandible using a Leica 1600 hard tissue microtome (Leica, Germany). Each block was sectioned with rotary abrasive paper to grind to a thickness of about 150 μm and then ground again to a final thickness of approximately 40 μm. Sections were cleaned with alcohol and stained with toluidine blue to observe the new bone formation around the bone graft using a U-LH300-3 microscope (Olympus, Japan) with Image-Pro software (Media Cybernetics, USA).

2.5 Statistical analysis

Data were analyzed using *t*-tests, one-way analysis of variance (ANOVA), and least significant differences (LSD) tests. A significance level of 0.05 was used in all statistical comparisons. All statistical analyses were performed with GraphPad Prism 6 software (GraphPad Prism 6, USA).

3 Results

3.1 Analysis of the surface morphology of the scaffolds

Photographs of the CHTS are shown in Fig. 4, and SEM images of the CTHS are shown in Fig. 5. The macroscopical shapes of both the scaffolds were similar. The mineral crystals were distributed densely throughout the collagen. SEM analysis of the CHTS and Bio-Oss Collagen showed that both the scaffolds shared similar structures, with a collagen fiber grid and homogeneously dispersed mineral crystals. The diameters of the mineral crystals were approximately 200–300 μm, and the CHTSs had smaller crystal diameters of about 100–150 μm.

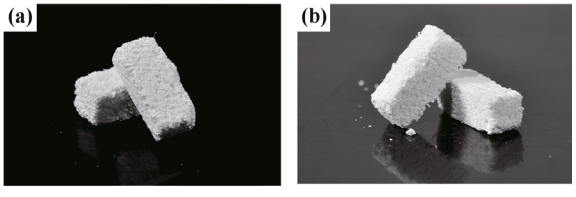

Fig. 4 Photographs of **(a)** the CHTS and **(b)** Bio-Oss Collagen.

3.2 Composition analysis

EDX spectra were obtained for the CHTS and Bio-Oss Collagen. One area containing both collagen fibers and crystals was selected randomly from each sample to perform plane scan analysis. The EDX spectra indicated that both samples had similar elements, including carbon, oxygen, and nitrogen, derived from the collagen, and calcium and phosphorus, derived from the bone granules. Compared with the Bio-Oss Collagen, the CHTS had a relatively lower molar ratio of calcium/phosphorus (12:7 versus 20:11, respectively) due to the presence of 50% TCP in the bone granules. A small amount of impurities, including sodium and chloride, were also be detected in both samples without significant differences. The FTIR spectra (Fig. 6(a)) showed typical peaks at 1030 and 602/566 cm^{-1}, indicative of the ν_3 and ν_4 vibrations of PO_4^{3-}. The peaks at 1547 and 1600 cm^{-1} were indicative of collagen (COO^-). Compared with the relatively low peaks of the Bio-Oss Collagen, the collagen component in the CHTS did not change significantly after the composite process. The XRD spectra (Fig. 6(b)) indicated the presence of significant peaks in the CHTS in the 2θ ranges of 23.4°–23.7° and 26.9°–27.4° (International Center for Diffraction Data, Joint Committee on Powder Diffraction Standards, CPDS No. 41-0487) and a much lower peak at 40.4°–40.9°, which indicated the TCP phase; the Bio-Oss Collagen did not have such features.

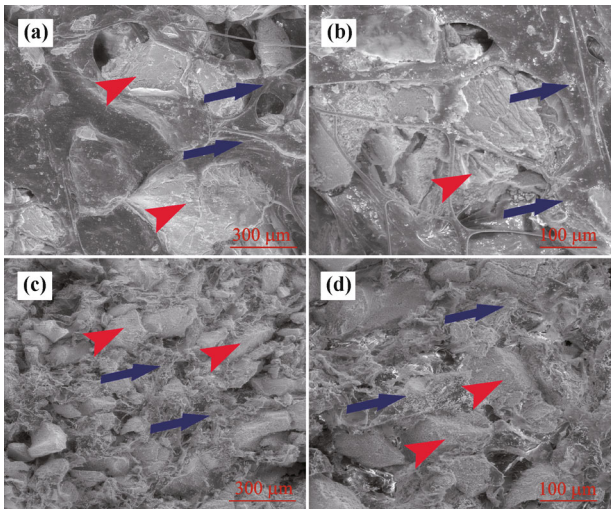

Fig. 5 SEM images of the CHTS and Bio-Oss Collagen: **(a)(b)** morphologies of Bio-Oss Collagen at 200× and 500× magnifications, respectively; **(c)(d)** morphologies of the CHTS at 200× and 500× magnifications, respectively. The blue arrows indicate collagen fibers, and the red arrows indicate mineral crystals.

3.3 MTT assays

In order to determine the cytotoxicity of the CHTS, MTT

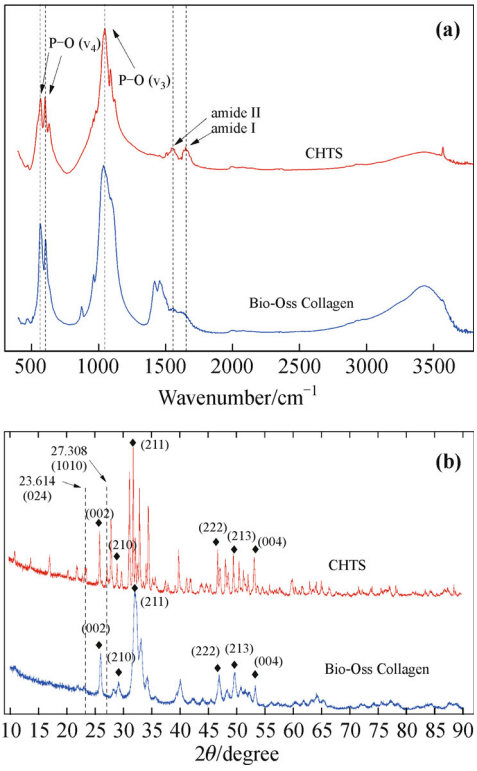

Fig. 6 **(a)** FTIR patterns of the CHTS and Bio-Oss Collagen. Both the CHTS and Bio-Oss Collagen shared the same organic and inorganic composition. Notes: red line, CHTS; blue line, Bio-Oss Collagen. The dashed lines indicate similar symbolic peaks in both groups: 1030 cm^{-1}, v_3 vibration of PO_4^{3-}; 602 and 566 cm^{-1}, v_4 vibration of PO_4^{3-}; 1547 cm^{-1}, amide II; 1600 cm^{-1}, amide I. **(b)** XRD spectra of the CHTS and Bio-Oss Collagen. Notes: red line, CHTS; blue line, Bio-Oss Collagen; rhombus symbols indicate the symbolic peaks of HA; dashed at 23.4°–23.7° and 26.9°–27.4° demonstrate the symbolic peaks of β-TCP in CHTS.

assays were performed in MC3T3-E1 cells cultured on both the CHTS and Bio-Oss Collagen. The growth curves (Fig. 7) showed that the overall growth tendency of both groups was similar from the third day to the fifth day. From the fifth day to the seventh day, cell proliferation on the CHTS was slightly higher than that on Bio-Oss Collagen. Notably, throughout the entire culture process, cell proliferation on both grafts was higher than that for the control group.

3.4 CBCT results

At 2 months after implantation, the controls showed significantly increased bone resorption for both height Bio-Oss ((2.11±0.61) mm *vs.* (0.85±0.46) and (1.25±0.74) mm, respectively; $p < 0.05$) and width ((1.14±0.59) mm *vs.* (0.54±0.50) and (0.67±0.30) mm, respectively; $p < 0.05$) compared with the CHTS and Bio-Oss Collagen

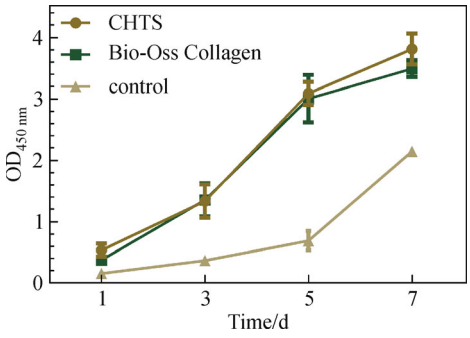

Fig. 7 The proliferation of MC3T3-E1 cell on CHTS and Bio-Oss Collagen.

(Fig. 8, Tables 1 and 2). Additionally, the density of alveolar bone in the control group ((1.14±0.59) mm) was significant lower than those in the other two groups. However, compared with Bio-Oss Collagen, the CHTS exhibited slightly lower bone resorption both vertically ((0.85±0.46) mm *vs.* (1.25±0.74) mm, respectively; p = 0.2103) and horizontally ((0.54±0.50) mm *vs.* (0.67±0.30) mm, respectively; p = 0.51). The bone density was slightly higher in the CHTS ((1566±194.66) HU *vs.* (1526±184.75) HU, respectively; p = 0.57). However, there were no significant differences.

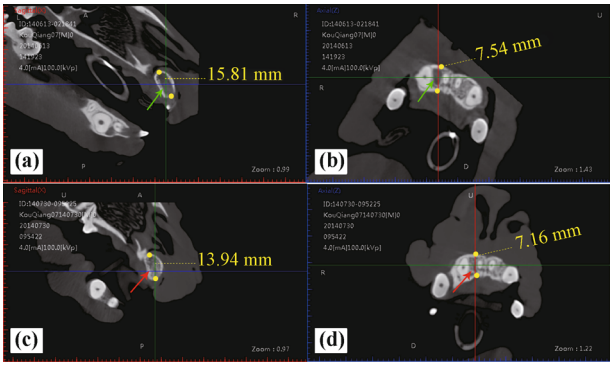

Fig. 8 CBCT slices at a typical site filled with CHTS: **(a)** Sagittal slice immediately after surgery; **(b)** Axial slice immediately after surgery; **(c)** Sagittal slice 2 months after surgery; **(d)** Axial slice 2 months after surgery. Notes: yellow points, markers of distance measurement; green lines, socket filled with CHTS; red lines, new bone formation in the socket.

3.5 Histological assessment

At 2 months after implantation, both the CHTS and Bio-Oss Collagengroups (Fig. 9) had some remaining mineral particles. However, the collagen fibers were degraded, and some mineral crystals were remodeled. Around the remaining mineral crystals, we found new woven bone matrix, as indicated by toluidine blue staining, with small

Table 1 Results of variables of alveolar bone preservation in Beagle dogs

Group	Variables		
	ΔHR /mm	ΔWR /mm	Density variation /HU
CHTS	0.85±0.46	0.54±0.50	1566±194.66
Bio-Oss Collagen	1.25±0.74	0.67±0.30	1526±184.75
Control	2.11±0.61	1.14±0.59	1118±108.91

Notes: ΔHR, variation in alveolar bone height; ΔWR, variation in alveolar bone width.

Table 2 Comparison of HR, WR, and density variations among groups

Comparison between groups	Significances of differences		
	ΔHR	ΔWR	Density variation
CHTS *vs.* Bio-Oss Collagen	$p = 0.21$	$p = 0.51$	$p = 0.57$
CHTS *vs.* Control	$^{**}p < 0.001$	$^{*}p < 0.05$	$^{**}p < 0.001$
Bio-Oss Collagen *vs.* Control	$^{*}p < 0.05$	$^{*}p < 0.05$	$^{**}p < 0.001$

Notes: $^{*}p < 0.05$, $^{**}p < 0.01$ by ANOVA and LSD tests.

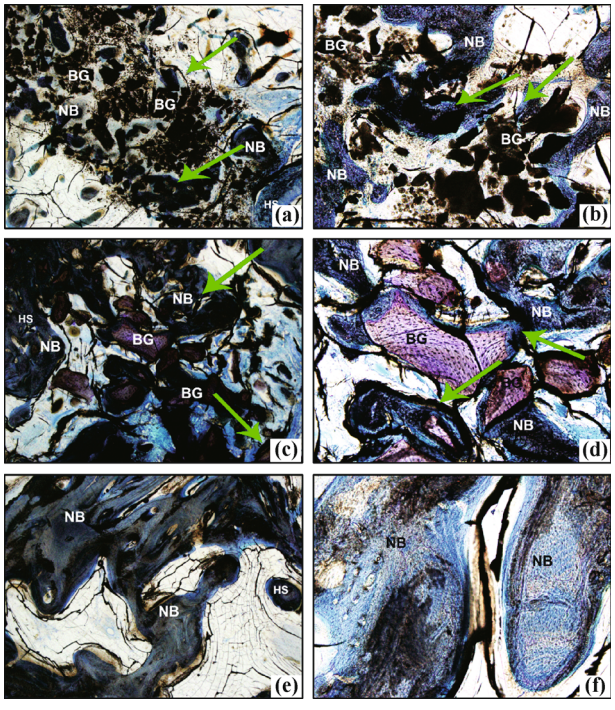

Fig. 9 Light microscopic images of toluidine blue-stained ground sections of mandibular bones at 8 weeks after implantation in mandibular defects: **(a)** CHTS, 10×; **(b)** CHTS, 20×; **(c)** Bio-Oss Collagen, 10×; **(d)** Bio-Oss Collagen, 20×; **(e)** Blank, 10×; **(f)** Blank, 20×. Notes: NB, new formed bone; BG, bone graft; HS, Haversian structure system; arrows, the boundary of the bone graft and new osteoid precipitation.

amounts of fiber tissues. Of the new osteoid precipitation, mature bone, with a regular arrangement of bone trabecula surrounded by several bone lacunas, was observed. Haversian structure systems were also detected around the area of the bone grafts. No histological indication of an inflammatory response was detected in either group. In the control group without any grafts, the density of the newly formed bone was less than that of the other two groups, and the proportion of fibrous tissue was also higher.

4 Discussion

In this study, we examined the features of a CHTS prepared using HA and β-TCP for bone regeneration *in vivo*. Our results showed that this CHTS showed good morphological and mechanical features comparable to those of a widely used biomaterial, Bio-Oss collagen. Thus, the CHTS may have applications in bone tissue engineering.

Conventional preparation approaches for collagen/HA/TCP composites include a supersaturated calcium phosphate aqueous solution or synthetic HA particles in order to achieve bone regeneration [41]. The disadvantages are obvious: the structure of the mineral crystals does not resemble the natural bone, which leads to poor mineralization of collagen, resulting in negative effects on the cells and tissue growth. However, bone particles from natural bone resources could remain in their native structure and chemical composition. Many studies have found that inorganic bovine bone shows better bone formation potential than other HA materials [43–46]. The classical method to disperse collagen is to dissolve the fibers in acid solution, such as acetic acid, which would cause inflammation in recipient areas due to the high acidity of the materials. In order to overcome this disadvantage, our composite approach used pure water as the solvent to dissolve the collagen with a homogenizer. Thus, the composite scaffold was expected to have a favorable pH of around 7. As a result, irritation from acid grafts could be avoided, providing a suitable environment for cell and tissue growth. Additionally, in order to improve the

mechanical properties of our scaffold, constant mechanical pressing was used rather than crosslinking with glutaraldehyde [47] or EDC/NHS [48], which can cause damage to the tissues and cells. Based on the above features, improved biocompatibility was achieved.

Bio-Oss Collagen, a novel bone graft material, has become increasingly common in clinical practice, particularly for alveolar ridge preservation [8,35,49]. Therefore, we used Bio-Oss Collagen as our control group to evaluate the efficacy and characteristics of our novel scaffolds. From SEM images and photographs of the CHTS and Bio-Oss Collagen samples, we found that the CHTS exhibited a similar arrangement of collagen and mineral crystals as the Bio-Oss Collagen. The CHTS had relatively smaller crystals and less porosity. Although pore sizes of 50–150 μm are suitable for tissue and cell growth [50], the rapid degradation of collagen fibers could provide suitable porosity owing to the pore structure of the mineral particles [51].

The EDX results showed that both groups shared similar elemental components. However, the calcium:phosphorus molar ratio of CHTS (8:5) was higher than 5:3 (the ratio of HA) and lower than 3:2 (the ratio of TCP) as a result of the coexistence of both components. However, the ratio of Bio-Oss Collagen was 20:11, which was lower than the ratio of HA owing to the presence of carbonatoapatite [52]. From the XRD spectrum, both HA and β-TCP could be detected in the CHTS. β-TCP, like HA, shares similar microsphere with natural bone [53] and biocompatibility, osteoconductivity and bioresorbable properties are also excellent [54–56]. It barely has the risk of rejection or infection [57] and there are many clinical researches confirming the safety and effectiveness of β-TCP [58–59]. The biodegradation rate and solubility of HA are low; thus, after combination with β-TCP, the composite would degrade and dissolve faster, which is suitable for tissue engineering applications [60]. β-TCP could also contribute to the differentiation of osteoblasts and subsequent bone formation, including the secretion and mineralization of ECM [61]. The high dissolution velocity of β-TCP could provide a high Ca^{2+} or PO_3^{4-} concentration environment, which could facilitate the osteogenic differentiation in many ways, such as the adsorption and release of bone forming factors [62] and adjustment of osteogenic cells phosphate metabolism and adenosine signaling [63]. Many researches also demonstrated that the high Ca^{2+} or PO_3^{4-} environment could promote the healing process of bone [64–66]. Therefore, the additional β-TCP in our CHTS could provide improved biological properties compared with the use of HA alone.

From the histological evaluation, both the CHTS and Bio-Oss Collagen showed excellent new bone formation. Some grafts had degraded. Around the residual granules of grafts, new forming woven bone trabecula could be clearly detected. Bone lacunas and Haversian structure systems could also be detected around the grafts. Although the results of the CHTS and Bio-Oss Collagen samples did not differ significantly from each other, likely owing to the small number of samples examined, new bone formation was obviously lower in the control than in the two treatment groups, suggesting that the CHTS and Bio-Oss Collagen promoted new bone growth.

Ridge preservation experiments can be an excellent simulation of the clinical use of bone grafts. From the results, the CHTS did not differ significantly in bone formation compared with the Bio-Oss Collagen, which has resulted in promising outcomes in clinical applications. In contrast to the significant bone resorption observed in the control group, the graft implant sites exhibited significantly less bone loss both in dimension and density. From CBCT imaging, we could evaluate the morphology of the alveolar bone and dynamic variations in more detail than by histological analysis alone. However, the CHTS had a relatively high standard deviation, particularly for variations in the width of the alveolar bone. This may have contributed to relatively high errors in location and measurement due to the limitations of CBCT and the software.

In all, compared with Bio-Oss Collagen, the golden standard in ridge preservation, the CHTS has similar morphology, microstructure but additional β-TCP, which could enable better osteogenesis effect. The results of cell toxicity and biological effects of CHTS did not demonstrate significant differences with Bio-Oss Collagen.

5 Conclusions

In the present study, we prepared a novel bone graft scaffold with calcined bovine bone particles and type-I collagen. The morphology and composition of the CHTS were similar to Bio-Oss Collagen, which has been used clinically. Furthermore, *in vitro* and *in vivo* biological evaluations showed that the CHTS promoted osteogenesis, similar to that of Bio-Oss Collagen. Therefore, our novel collagen/HA/TCP scaffold had excellent biological properties and may have applications in clinical practice.

Acknowledgements This study was supported by funds from the National Natural Science Foundation of China (NSFC; Grant No. 51572144) and the Science Foundation of Beijing Research (Grant No. Z121100005212009).

References

[1] Nussbaum B, Carrel R. The behavior modification of a dentally disabled child. ASDC Journal of Dentistry for Children, 1976, 43 (4): 255–261

[2] Chen S T, Buser D. Clinical and esthetic outcomes of implants placed in postextraction sites. The International Journal of Oral & Maxillofacial Implants, 2009, 24(Suppl): 186–217

[3] Li X, Liu H, Niu X, et al. The use of carbon nanotubes to induce osteogenic differentiation of human adipose-derived MSCs *in vitro* and ectopic bone formation *in vivo*. Biomaterials, 2012, 33 (19): 4818–4827

[4] Shao S, Li B, Xue H M, et al. Effects of alveolar ridge preservation on delayed implant osseointegration. International Journal of Clinical and Experimental Medicine, 2015, 8(7): 10773–10778

[5] Tan W L, Wong T L, Wong M C, et al. A systematic review of post-extractional alveolar hard and soft tissue dimensional changes in humans. Clinical Oral Implants Research, 2012, 23 (Suppl 5): 1–21

[6] Araújo M G, Lindhe J. Dimensional ridge alterations following tooth extraction. An experimental study in the dog. Journal of Clinical Periodontology, 2005, 32(2): 212–218

[7] Van der Weijden F, Dell'Acqua F, Slot D E. Alveolar bone dimensional changes of post-extraction sockets in humans: a systematic review. Journal of Clinical Periodontology, 2009, 36 (12): 1048–1058

[8] Tomlin E M, Nelson S J, Rossmann J A. Ridge preservation for implant therapy: a review of the literature. The Open Dentistry Journal, 2014, 8(1): 66–76

[9] Park Y S, Kim S, Oh S H, et al. Comparison of alveolar ridge preservation methods using three-dimensional micro-computed tomographic analysis and two-dimensional histometric evaluation. Imaging Science in Dentistry, 2014, 44(2): 143–148

[10] Araújo M G, Lindhe J. Ridge preservation with the use of Bio-Oss collagen: A 6-month study in the dog. Clinical Oral Implants Research, 2009, 20(5): 433–440

[11] Ashman A. Ridge preservation — the future practice of dentistry. Dental Economics-Oral Hygiene, 1995, 85(8): 80, 82–83

[12] Yamasaki N, Hirao M, Nanno K, et al. A comparative assessment of synthetic ceramic bone substitutes with different composition and microstructure in rabbit femoral condyle model. Journal of Biomedical Materials Research Part B: Applied Biomaterials, 2009, 91(2): 788–798

[13] Schliephake H, Kage T. Enhancement of bone regeneration using resorbable ceramics and a polymer–ceramic composite material. Journal of Biomedical Materials Research, 2001, 56(1): 128–136

[14] Sakai K, Hashimoto Y, Baba S, et al. Effects on bone regeneration when collagen model polypeptides are combined with various sizes of α-tricalcium phosphate particles. Dental Materials Journal, 2011, 30(6): 913–922

[15] Li X, Wang L, Fan Y, et al. Nanostructured scaffolds for bone tissue engineering. Journal of Biomedical Materials Research Part A, 2013, 101(8): 2424–2435

[16] Kihara H, Shiota M, Yamashita Y, et al. Biodegradation process of α-TCP particles and new bone formation in a rabbit cranial defect model. Journal of Biomedical Materials Research Part B: Applied Biomaterials, 2006, 79(2): 284–291

[17] Li Q, Zhou G, Yu X, et al. A novel deproteinized bovine bone scaffold containing chitosan microspheres for controlled delivery of BMP-2. In: Liu H W, Wang G, Zhang G W, eds. Applied Mechanics and Materials, 2014, 187–190

[18] Zhou Y, Yao H, Wang J, et al. Greener synthesis of electrospun collagen/hydroxyapatite composite fibers with an excellent microstructure for bone tissue engineering. International Journal of Nanomedicine, 2015, 10: 3203–3215

[19] Do A V, Khorsand B, Geary S M, et al. 3D printing of scaffolds for tissue regeneration applications. Advanced Healthcare Materials, 2015, 4(12): 1742–1762

[20] Li Q, Zhou G, Wang T, et al. Investigations into the biocompatibility of nanohydroxyapatite coated magnetic nanoparticles under magnetic situation. Journal of Nanomaterials – Special Issue on Biocompatibility and Toxicity of Nanobiomaterials 2014, 2015, 835604 (10 pages)

[21] MacMillan A K, Lamberti F V, Moulton J N, et al. Similar healthy osteoclast and osteoblast activity on nanocrystalline hydroxyapatite and nanoparticles of tri-calcium phosphate compared to natural bone. International Journal of Nanomedicine, 2014, 9: 5627–5637

[22] Mate S D V J, Calvo G J, Ramirez F M, et al. *In vivo* behavior of hydroxyapatite/β-TCP/collagen scaffold in animal model. Histological, histomorphometrical, radiological, and SEM analysis at 15, 30, and 60 days. Clinical Oral Implants Research, doi: 10.1111/clr.12656 (in press)

[23] Lim H C, Zhang M L, Lee J S, et al. Effect of different hydroxyapatite:β-tricalcium phosphate ratios on the osteoconductivity of biphasic calcium phosphate in the rabbit sinus model. The International Journal of Oral & Maxillofacial Implants, 2015, 30 (1): 65–72

[24] Huang Y, Zhou G, Zheng L, et al. Micro-/nano-sized hydroxyapatite directs differentiation of rat bone marrow derived mesenchymal stem cells towards an osteoblast lineage. Nanoscale, 2012, 4(7): 2484–2490

[25] Vo T N, Kasper F K, Mikos A G. Strategies for controlled delivery of growth factors and cells for bone regeneration. Advanced Drug Delivery Reviews, 2012, 64(12): 1292–1309

[26] Matsuno T, Nakamura T, Kuremoto K, et al. Development of β-tricalcium phosphate/collagen sponge composite for bone regeneration. Dental Materials Journal, 2006, 25(1): 138–144

[27] Li X, Huang Y, Zheng L, et al. Effect of substrate stiffness on the functions of rat bone marrow and adipose tissue derived mesenchymal stem cells *in vitro*. Journal of Biomedical Materials Research Part A, 2014, 102(4): 1092–1101

[28] Carlson G A, Dragoo J L, Samimi B, et al. Bacteriostatic properties of biomatrices against common orthopaedic pathogens. Biochemical and Biophysical Research Communications, 2004, 321(2): 472–478

[29] Hiraoka Y, Kimura Y, Ueda H, et al. Fabrication and biocompatibility of collagen sponge reinforced with poly(glycolic acid) fiber. Tissue Engineering, 2003, 9(6): 1101–1112

[30] Li X, Yang Y, Fan Y, et al. Biocomposites reinforced by fibers or tubes as scaffolds for tissue engineering or regenerative medicine. Journal of Biomedical Materials Research Part A, 2014, 102(5): 1580–1594

[31] Yamauchi K, Goda T, Takeuchi N, et al. Preparation of collagen/calcium phosphate multilayer sheet using enzymatic mineralization. Biomaterials, 2004, 25(24): 5481–5489

[32] Lawson A C, Czernuszka J T. Collagen–calcium phosphate composites. Proceedings of the Institution of Mechanical Engineers Part H: Journal of Engineering in Medicine, 1998, 212(6): 413–425

[33] Lee H R, Kim H J, Ko J S, et al. Comparative characteristics of porous bioceramics for an osteogenic response *in vitro* and *in vivo*. PLoS ONE, 2013, 8(12): e84272

[34] Wong R W, Rabie A B. Effect of bio-oss collagen and collagen matrix on bone formation. The Open Biomedical Engineering Journal, 2010, 4(1): 71–76

[35] Palachur D, Prabhakara Rao K V, Murthy K R, et al. A comparative evaluation of bovine-derived xenograft (Bio-Oss Collagen) and type I collagen membrane (Bio-Gide) with bovine-derived xenograft (Bio-Oss Collagen) and fibrin fibronectin sealing system (TISSEEL) in the treatment of intrabony defects: A clinico-radiographic study. Journal of Indian Society of Periodontology, 2014, 18(3): 336–343

[36] Nevins M L, Camelo M, Lynch S E, et al. Evaluation of periodontal regeneration following grafting intrabony defects with bio-oss collagen: a human histologic report. The International Journal of Periodontics & Restorative Dentistry, 2003, 23(1): 9–17

[37] Cardaropoli D, Re S, Manuzzi W, et al. Bio-Oss collagen and orthodontic movement for the treatment of infrabony defects in the esthetic zone. The International Journal of Periodontics & Restorative Dentistry, 2006, 26(6): 553–559

[38] Heinemann F, Hasan I, Schwahn C, et al. Bone level change of extraction sockets with Bio-Oss collagen and implant placement: a clinical study. Annals of Anatomy, 2012, 194(6): 508–512

[39] Li Q, Zhou G, Yu X, et al. Porous deproteinized bovine bone scaffold with three-dimensional localized drug delivery system using chitosan microspheres. Biomedical Engineering Online, 2015, 14(1): 33

[40] Hosseinzadeh E, Davarpanah M, Hassanzadeh Nemati N, et al. Fabrication of a hard tissue replacement using natural hydroxyapatite derived from bovine bones by thermal decomposition method. International Journal of Organ Transplantation Medicine, 2014, 5(1): 23–31

[41] Antebi B, Cheng X, Harris J N, et al. Biomimetic collagen–hydroxyapatite composite fabricated via a novel perfusion-flow mineralization technique. Tissue Engineering Part C: Methods, 2013, 19(7): 487–496

[42] Salomó-Coll O, Maté-Sánchez de Val J E, Ramírez-Fernandez M P, et al. Topical applications of vitamin D on implant surface for bone-to-implant contact enhance: a pilot study in dogs part II. Clinical Oral Implants Research, doi: 10.1111/clr.12707 (in press)

[43] Berglundh T, Lindhe J. Healing around implants placed in bone defects treated with Bio-Oss. An experimental study in the dog. Clinical Oral Implants Research, 1997, 8(2): 117–124

[44] Piattelli M, Favero G A, Scarano A, et al. Bone reactions to anorganic bovine bone (Bio-Oss) used in sinus augmentation procedures: a histologic long-term report of 20 cases in humans. The International Journal of Oral & Maxillofacial Implants, 1999, 14(6): 835–840

[45] Carmagnola D, Adriaens P, Berglundh T. Healing of human extraction sockets filled with Bio-Oss. Clinical Oral Implants Research, 2003, 14(2): 137–143

[46] Caubet J, Petzold C, Sáez-Torres C, et al. Sinus graft with safescraper: 5-year results. Journal of Oral and Maxillofacial Surgery, 2011, 69(2): 482–490

[47] Chandran P L, Paik D C, Holmes J W. Structural mechanism for alteration of collagen gel mechanics by glutaraldehyde cross-linking. Connective Tissue Research, 2012, 53(4): 285–297

[48] Davidenko N, Schuster C F, Bax D V, et al. Control of crosslinking for tailoring collagen-based scaffolds stability and mechanics. Acta Biomaterialia, 2015, 25: 131–142

[49] Panday V, Upadhyaya V, Berwal V, et al. Comparative evalution of G bone (hydroxyapatite) and G-graft (hydroxyapatite with collagen) as bone graft material in mandibular III molar extraction socket. Journal of Clinical and Diagnostic Research, 2015, 9(3): ZC48–ZC52

[50] Gérard C, Doillon C J. Facilitating tissue infiltration and angiogenesis in a tubular collagen scaffold. Journal of Biomedical

Materials Research Part A, 2010, 93(2): 615–624

[51] Chen P Y, Toroian D, Price P A, et al. Minerals form a continuum phase in mature cancellous bone. Calcified Tissue International, 2011, 88(5): 351–361

[52] Esposito M, Grusovin M G, Kwan S, et al. Interventions for replacing missing teeth: bone augmentation techniques for dental implant treatment. The Cochrane Database of Systematic Reviews, 2008, (3): CD003607

[53] Lee J H, Kim J, Baek H R, et al. Fabrication of an rhBMP-2 loaded porous β-TCP microsphere-hyaluronic acid-based powder gel composite and evaluation of implant osseointegration. Journal of Materials Science: Materials in Medicine, 2014, 25(9): 2141–2151

[54] Hench L L, Polak J M. Third-generation biomedical materials. Science, 2002, 295(5557): 1014–1017

[55] Wang L, Hu Y Y, Wang Z, et al. Flow perfusion culture of human fetal bone cells in large β-tricalcium phosphate scaffold with controlled architecture. Journal of Biomedical Materials Research Part A, 2009, 91(1): 102–113

[56] Yu H D, Zhang Z Y, Win K Y, et al. Bioinspired fabrication of 3D hierarchical porous nanomicrostructures of calcium carbonate for bone regeneration. Chemical Communications, 2010, 46(35): 6578–6580

[57] Wu W, Chen X, Mao T, et al. Bone marrow-derived osteoblasts seeded into porous β-tricalcium phosphate to repair segmental defect in canine's mandibula. Turkish Journal of Trauma & Emergency Surgery, 2006, 12(4): 268–276

[58] McAndrew M P, Gorman P W, Lange T A. Tricalcium phosphate as a bone graft substitute in trauma: preliminary report. Journal of Orthopaedic Trauma, 1988, 2(4): 333–339

[59] Simunek A, Kopecka D, Somanathan R V, et al. Deproteinized bovine bone versus β-tricalcium phosphate in sinus augmentation surgery: a comparative histologic and histomorphometric study. The International Journal of Oral & Maxillofacial Implants, 2008, 23(5): 935–942

[60] Shavandi A, Bekhit A D, Ali M A, et al. Development and characterization of hydroxyapatite/β-TCP/chitosan composites for tissue engineering applications. Materials Science and Engineering C, 2015, 56: 481–493

[61] Arahira T, Todo M. Effects of proliferation and differentiation of mesenchymal stem cells on compressive mechanical behavior of collagen/β-TCP composite scaffold. Journal of the Mechanical Behavior of Biomedical Materials, 2014, 39: 218–230

[62] Autefage H, Briand-Mésange F, Cazalbou S, et al. Adsorption and release of BMP-2 on nanocrystalline apatite-coated and uncoated hydroxyapatite/β-tricalcium phosphate porous ceramics. Journal of Biomedical Materials Research Part B, 2009, 91(2): 706–715

[63] Shih Y R, Hwang Y, Phadke A, et al. Calcium phosphate-bearing matrices induce osteogenic differentiation of stem cells through adenosine signaling. Proceedings of the National Academy of Sciences of the United States of America, 2014, 111(3): 990–995

[64] Li X, van Blitterswijk C A, Feng Q, et al. The effect of calcium phosphate microstructure on bone-related cells *in vitro*. Biomaterials, 2008, 29(23): 3306–3316

[65] Li X, Liu H, Niu X, et al. Osteogenic differentiation of human adipose-derived stem cells induced by osteoinductive calcium phosphate ceramics. Journal of Biomedical Materials Research Part B, 2011, 97(1): 10–19

[66] Hoppe A, Güldal N S, Boccaccini A R. A review of the biological response to ionic dissolution products from bioactive glasses and glass–ceramics. Biomaterials, 2011, 32(11): 2757–2774